A loss of memory in stratified momentum wakes

Patrice Meunier[a] and Geoffrey R. Spedding
Department of Aerospace and Mechanical Engineering, University of Southern California, Los Angeles, California 90089-1191

(Received 29 April 2003; accepted 8 October 2003; published online 24 December 2003)

In this paper we compare the wakes of various bluff bodies in a stratified fluid at moderately high Froude numbers ($F \equiv 2U_B/ND > 8$) and Reynolds numbers (Re$\approx$5000). The size and amplitude of the long-lasting wakes clearly depend on the shape of the bluff body, the wake width being small for a streamlined object and large for an object with sharp edges. However, the wake width can be collapsed when it is normalized by an effective diameter based on the drag force, often called the momentum thickness. General laws for the wake width, the velocity defect, and the Strouhal number are thus deduced and fit the data well. Finally, the cross-fluctuations of the velocity and the turbulent kinetic energy are analyzed. Their amplitudes and widths are proportional to those of the mean profile. Thus, the wake remembers only the momentum flux given by the bluff body to the fluid and not any other aspects of its geometry. © *2004 American Institute of Physics.*
[DOI: 10.1063/1.1630053]

I. INTRODUCTION

Interest in stratified flows comes primarily from geophysical applications, due to the stratification of atmosphere and oceans. One focus concerns the effect of a stable stratification on homogeneous turbulence,[1–3] while another concentrates on the evolution of wakes in stratified flows,[4,5] especially for spheres.[6–8] All these results were obtained in the presence of a strong stratification, i.e., for small Froude numbers. For the wake flows, the Froude number is defined by $F \equiv 2U_B/ND$, where D is the diameter of the body, U_B the towing velocity, and $N=(g/\rho)^{1/2}(\partial\rho/\partial z)^{1/2}$ the buoyancy (or Brunt–Väisälä) frequency. For high Froude numbers, the effect of the stratification is negligible at early stages. However, since in wakes and in decaying turbulence the velocity decreases with time, the local Froude number will eventually approach 1 and the buoyancy effects can no longer be neglected. A global mechanism for weakly stratified wakes was proposed[9] for spheres at high Reynolds numbers (Re$>$4000) and can be decomposed into three stages.

In the first stage, the wake possess high velocities and creates a three-dimensional (3-D) flow, equivalent to that of a nonstratified fluid.[10–12] The velocity follows a power law in time scaling with a decay exponent $-2/3$ and the duration ($N\Delta t \approx 2$) of this stage is fairly independent of the type of wake, in agreement with the general results of stratified turbulence.[3] In units of downstream distance, the duration of this stage increases with F ($\Delta x/D \approx F$) and the second stage will never occur for infinite Froude numbers, leaving the wake in a three-dimensional state as in the case of nonstratified fluids.

The second stage starts as soon as the buoyancy cannot be neglected, which removes vertical velocities. The flow becomes more laminar and organizes into flat horizontal vortices. The fluctuations of density, created by the first stage, collapse since they are no longer maintained by vertical velocity fluctuations and potential energy is transformed back into kinetic energy. This mechanism limits the decay of the velocity defect, whose exponent has been determined experimentally to be close to -0.25. This stage is a nonequilibrium phase (NEQ), where the flow transitions from the initial 3-D regime to a last stage.

In the third stage, the wake begins to diffuse in the vertical direction again,[13] perhaps due to some kind of Ekman pumping. This enhances the decay of the velocity defect, although the wake is still very coherent. The decay exponent was found to be close to the 3-D case ($-2/3$) and not to the 2-D case ($-1/2$), although the flow is very close to two-dimensional. This regime is thus named quasi-two-dimensional (Q2-D).

The presence of the second stage slows the decay of the velocity defect and the stratified flows are thus known to preserve the wake for longer times than in the absence of stratification. In nonstratified flows, Bevilaqua and Lykoudis[10] have shown that there can be a memory of the initial conditions in turbulent bluff body wakes, i.e., that the structure of the flow depends on the shape of the bluff body. The objective of this paper is to examine the effect of body geometry on the intermediate and late wake structure. The goal is both to determine the possibility of a long-term memory in the stratified wake, and to determine one specific set of rescaling parameters if such parameters are found.

II. EXPERIMENT AND ANALYSIS

The experiment has been described in detail in previous papers,[8,9] and only the main features of the apparatus, and of the data acquisition and treatment are outlined here.

[a]Present address: Institut de Recherche sur les Phénomènes Hors Équilibre, 49 rue F. Joliot-Curie, B.P. 146, F-13384 Marseille Cedex 13, France.

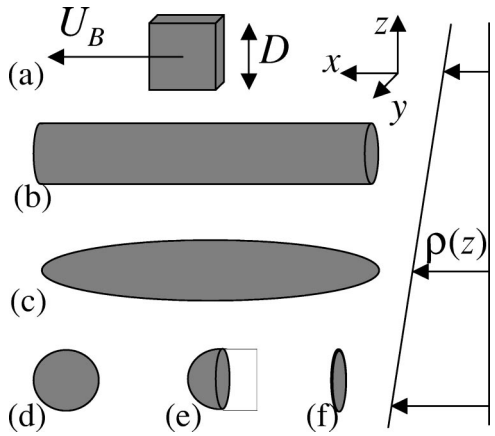

FIG. 1. Schematic of a cube (a), a 6:1 cylinder (b), a 6:1 prolate spheroid (c), a sphere (d), a hemisphere (e), and a disk (f) towed at a velocity U_B in a stably stratified fluid.

A. Experimental setup

The tank of dimensions 380×244 cm^2 is filled up to a height of 20 cm with stably stratified salted water, whose linear density gradient creates a buoyancy frequency $N=(-g/\rho_0)^{1/2}(\partial\rho/\partial z)^{1/2}\approx 2\ \mathrm{s}^{-1}$. A bluff body is towed at mid-height of the tank between three guide cables, using three thin towing cables under a strong tension. This setup prevents any oscillation of the body and the disturbances from the wire wakes are negligible. The bluff body is towed at a velocity U_B along the x axis, while the z axis is aligned with the vertical, as shown in Fig. 1. To investigate the influence of the shape of the body, several objects are used: a sphere for comparison with previous results, two slender objects such as a 6:1 cylinder and a 6:1 prolate spheroid, a disk perpendicular to the towing direction, a hemisphere whose flat face is turned backward and a cube with edges parallel to the axis (see Fig. 1). The diameter D of the bluff bodies (D being the size of the edges for the cube) was equal to 1.3 or 2.5 cm. These three quantities lead to two nondimensional parameters: the Froude number $F\equiv 2U_B/ND$ was equal to 8 or 32 and the Reynolds number $\mathrm{Re}\equiv U_B D/\nu$ (ν is the kinematic viscosity) was always close to 5000. In this paper we focus on the shape of the bluff body, which can be characterized by a third parameter A,[14] or by measuring its drag coefficient in a nonstratified fluid.

B. Definition of the flow characteristics

The evolution of the wake is analyzed by customized particle image velocimetry measurements, by introducing small reflecting particles with the density of the middle isopycnal. Digital images are analyzed by the correlation image velocimetry algorithm[15] to estimate instantaneous horizontal velocity fields (u,v) with dimensions 79×56 cm^2. The vertical component of the vorticity $\omega_z=\partial v/\partial x-\partial u/\partial y$ is shown in Fig. 2 for the prolate spheroid as a function of time. The vorticity fields are qualitatively similar for other objects (the case of the sphere being extensively shown[8,9]) and reveal the presence of coherent alternate vortices, whose size increases due to merging. Such a behavior has been already revealed by dye visualizations for various bluff bodies[4] and for a moving momentum source.[16]

Mean profiles are analyzed in Sec. III A. Second, the longitudinal distance λ_x between two vortices of the same sign defines a Strouhal number ($\mathrm{St}=D/\lambda_x$), which is compared to an extensive previous analysis on spheres.[17] The fluctuations of the velocity (u',v') are analyzed in Sec. IV.

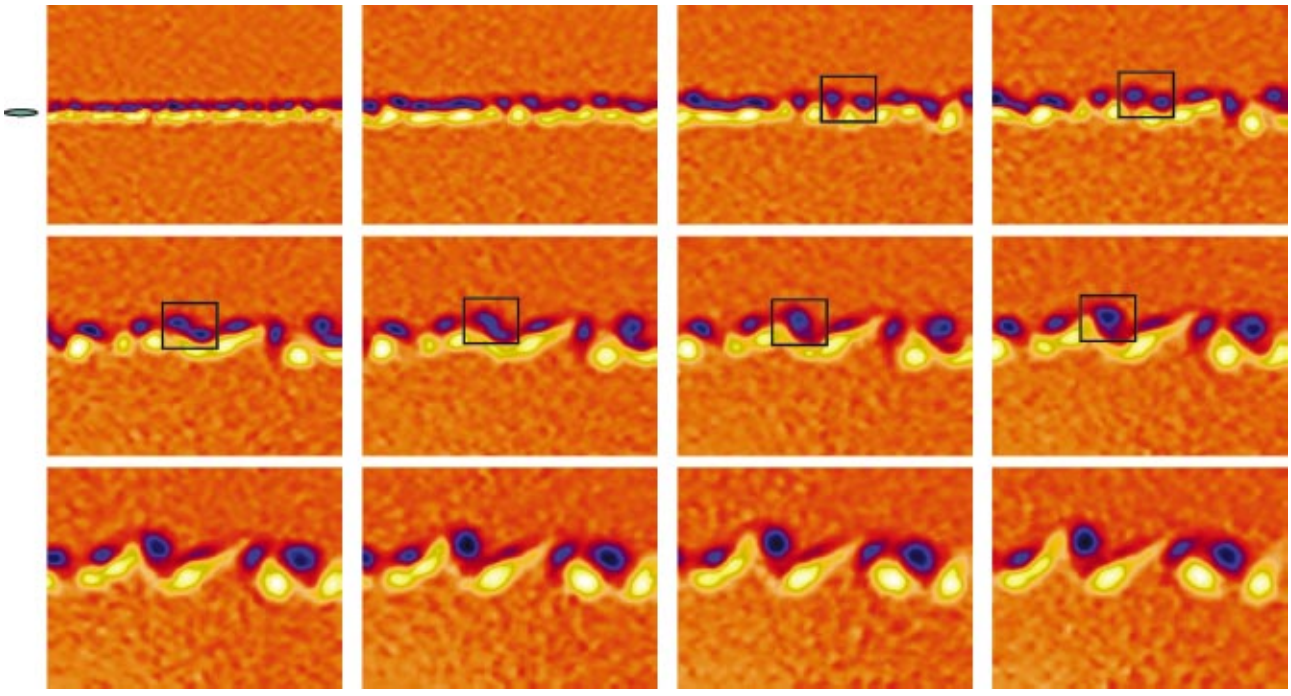

FIG. 2. (Color) The time series of the vertical vorticity distribution, $\omega_z(x,y,Nt)$ for the slender spheroid. $F=32$, $\mathrm{Re}=5.8\times10^3$, and the time steps are equally spaced from $Nt=5$ (top left) to $Nt=300$ (bottom right). The observation area has dimensions 61×43 D and the spheroid passed from right to left through it.

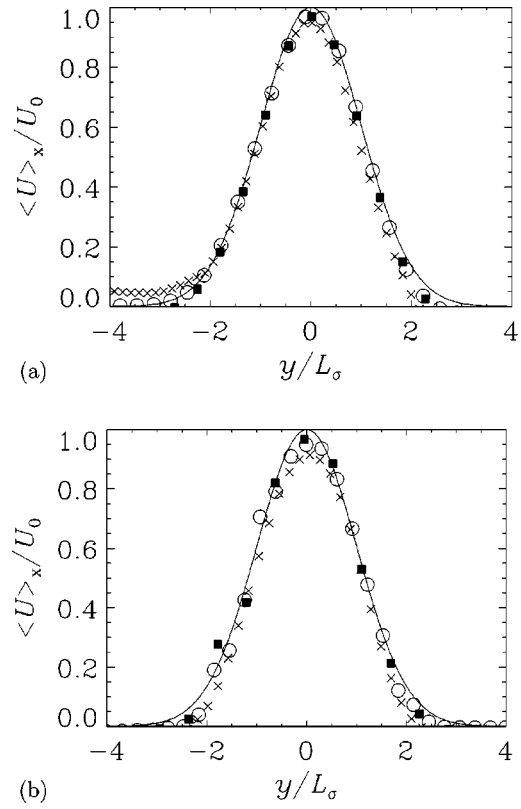

FIG. 3. Mean profiles of the streamwise velocity behind (a) the slender spheroid and (b) the cylinder. The averages are calculated on the global field of view for a downstream distance $x/D=170$ (■), $x/D=1000$ (○), and $x/D=5000$ (×). $F=32$ and Re≈5000. The solid lines correspond to the nondimensionalized Gaussian profile defined by Eq. (1).

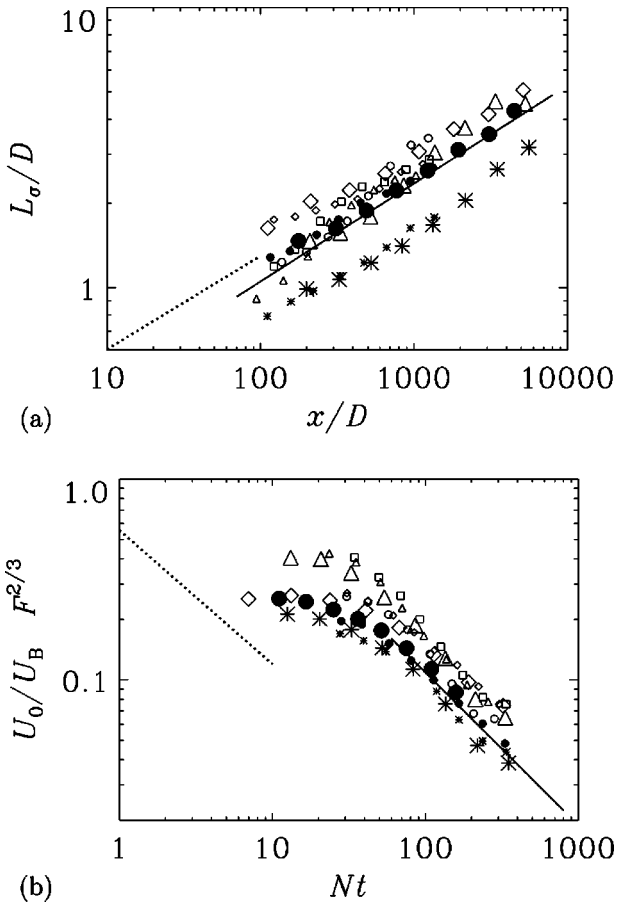

FIG. 4. Temporal evolution of the wake width L_σ (a) and of the velocity defect U_0 (b), defined by Eq. (1). The objects are a sphere (●), a slender spheroid (∗), a cylinder (△), a disc (◇), a cube (□), and a hemisphere (○). Small symbols correspond to $F=8$ and large symbols to $F=32$. Re≈5000. The solid line corresponds to the case of a sphere (Ref. 9) and the dotted line to a nonstratified sphere wake (Ref. 10).

In this towed configuration, mean quantities are obtained by averages over the streamwise direction and are plotted as a function of time Nt or as a function of the downstream distance x/D (they two are simply linked by $x/D=Nt\,F/2$).

III. A LOSS OF MEMORY?

Although the wakes are qualitatively similar, some quantitative differences have been observed and we will explain in this section how to collapse the results obtained on these various objects.

A. Mean profiles

Mean profiles of the streamwise velocity have been measured as a function of the downstream distance for each bluff body. They are shown in Fig. 3 for the slender spheroid and for the cylinder. The profiles are very close to Gaussian over a large band of downstream distances, in agreement with the theory of self preserving three-dimensional wakes.[18] They can be fitted by a Gaussian function,

$$U(y)=\langle u\rangle_x(y)=U_0 e^{-y^2/2L_\sigma^2}, \tag{1}$$

characterized by amplitude U_0 and wake half-width L_σ.

The wake width L_σ is plotted in Fig. 4(a) as a function of downstream distance for the various objects.

For the sphere, the growth has an exponent of $+0.35$ and is in very good agreement with the previous results[9] (solid line), also shown to be close to the nonstratified case. The magnitude of the wake width seems to be sensitive to the shape of the bluff body. For a streamlined object like the slender spheroid, the wake width is 30% smaller, but the growth rate is similar. On the contrary, for objects with sharp edges (open symbols in Fig. 4), the wake is slightly larger (up to 20%) while the growth rate is again very similar.

The same analysis can be performed for the amplitude U_0 of the mean profile, shown in Fig. 4(b). Spedding[9] has shown that the amplitude should be plotted as a function of time Nt to collapse all the results at different Froude numbers in the NEQ regime. Figure 4(b) shows that the results collapse for different Froude numbers in these coordinates and that they are in very good agreement with the results of Ref. 9. The velocity is much higher than in the absence of stratification due to the low decay in the NEQ regime. For a streamlined object such as the spheroid, the amplitude of the mean profile is smaller. The presence of sharp edges on the bluff body increases the amplitude. As for the wake width, the growth/decay rates appear to be independent of the shape of the bluff body.

The results indicate that the growth mechanism of the wake might be identical for all bluff bodies and that the

TABLE I. Values of the effective diameter D_{eff} for various bluff bodies defined by Eq. (2) using the drag force. The values for the drag force are taken from Blevins (Ref. 19).

Bluff body	Spheroid	Sphere	Hemisphere	Cylinder	Disk	Cube
D_{eff}/D	0.30	0.45	0.46	0.65	0.74	0.82

shape of the bluff body only changes the scaling of the flow. We thus seek to explain these differences by finding another length scale, which takes into account the shapes of the objects.

B. Toward universality

It seems intuitive that a streamlined object should have a narrower and slower wake than the sphere, since less fluid is entrained behind it. On the other hand, the presence of sharp edges modifies the vortex shedding and might create bigger vortices, leading to a thicker and more energetic wake. The appropriate length scale of the problem seems to be linked to the section of entrained fluid. The wakes of complex objects are not very well known in the literature and we would like to use a better defined quantity. Such a length scale has already been used theoretically by Tennekes and Lumley,[18] who showed that the momentum of the entrained fluid per unit time is exactly equal to the drag force on the object. If the entrained fluid has a section of diameter D_{eff}, also called the momentum thickness, inside which the velocity is U_B and zero outside, then the drag force is

$$F_{\text{drag}} = \rho_0 \frac{\pi D_{\text{eff}}^2}{4} U_B^2. \tag{2}$$

This definition of an effective diameter D_{eff} is very convenient since the drag force has been extensively studied in the literature.[19] It is thus easy to calculate the effective diameter for various shapes of bluff bodies, as shown in Table I, where the results of Blevins[19] are used. It can be noted that for axisymmetric bluff bodies the drag coefficient c_D is defined by

$$F_{\text{drag}} = \frac{1}{2} c_D \rho_0 \frac{\pi D^2}{4} U_B^2, \tag{3}$$

leading to a simplified definition of the effective diameter: $D_{\text{eff}} = D\sqrt{c_D/2}$. Figure 5(a) shows the wake width normalized by the effective diameter as a function of the downstream distance (similarly normalized). A reasonable collapse of the results is obtained [cf. Fig. 4(a)], indicating that the effective diameter is a more relevant length scale than the physical diameter of the bluff body. Moreover, the results for the amplitude U_0 also collapse when the Froude number is defined using the effective diameter ($F_{\text{eff}} = 2U_B/ND_{\text{eff}}$). It can be noted that the same collapse occurs when plotting U_0/U_B as a function of x/D_{eff}, since the two representations are equivalent in the Q2-D stage (but not in the NEQ regime).

The wake geometry depends only on the amount of entrained fluid and not on the real shape of the bluff body. The same conclusion was recently obtained by Voropayev and Smirnov[16] in the case of a towed jet, by introducing the same length scale as in (2).

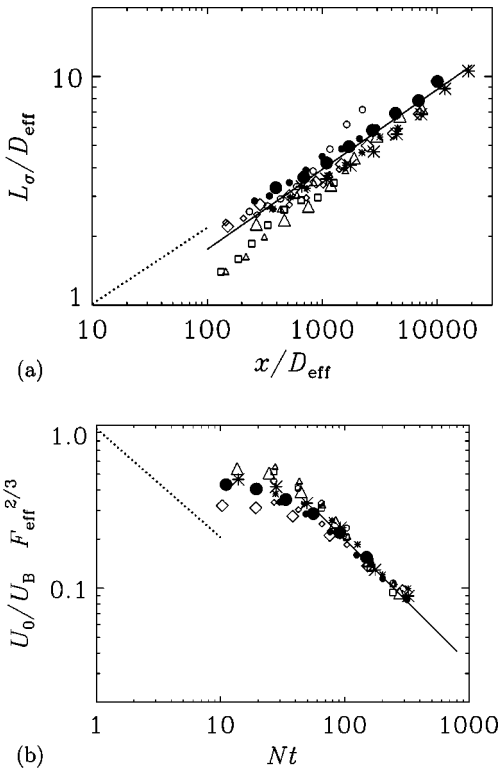

FIG. 5. Temporal evolution of the wake width L_σ (a) and of the velocity defect U_0 (b), defined by Eq. (1). Quantities are normalized using the effective diameter D_{eff} defined in Eq. (2) using the drag force. Symbols are as in Fig. 4. The solid line corresponds to the case of a sphere (Ref. 9) and the dotted line to a nonstratified sphere wake (Ref. 10).

The collapse of the results allows a prediction of the wake width and amplitude for any bluff body, based only on its drag coefficient in a nonstratified fluid. Universal laws are found empirically to be

$$L_\sigma/D_{\text{eff}} = 0.35(x/D_{\text{eff}})^{0.35}, \tag{4}$$

$$U_0/U_B F_{\text{eff}}^{2/3} = 6.6(Nt)^{-0.76}. \tag{5}$$

The results collapse very well in these experiments since the bluff bodies were moderately modified. When the nature of the forcing from the body to the fluid is rather different, e.g., when a large force doublet or force quadruplet is added, the results might be affected more strongly. However, Voropayev *et al.*[20] studied a maneuvering self-propelled body, and found that even if the momentum is small compared to the force doublet, the final stage of the flow is mainly determined by the momentum, consistent with the differing decay rates derived theoretically for a laminar[21] or turbulent[18] nonstratified wake. Consequently, the relationships (4) and (5) might be quite general.

C. Strouhal number

The Strouhal number has been shown to decay with downstream distance due to merging of like-signed vortices[17] with constant exponent $-1/3$. This is the inverse of the

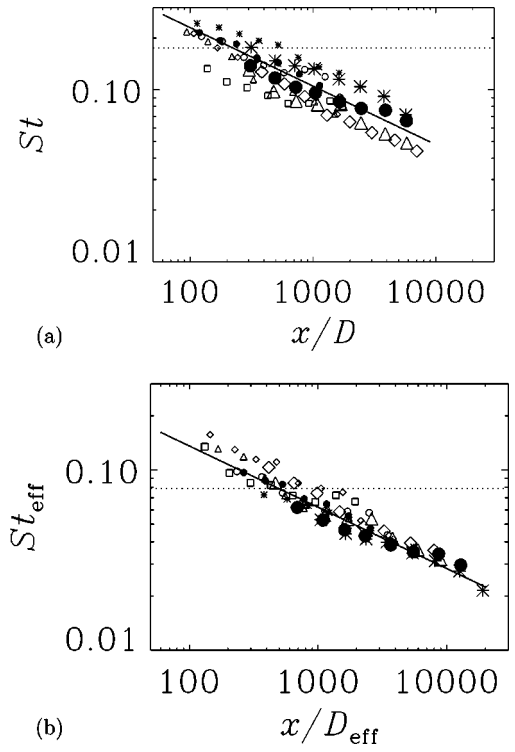

FIG. 6. The Strouhal number obtained by the mean streamwise distance between vortices. Quantities are normalized using (a) the real diameter D and (b) the effective diameter D_{eff} for a sphere (●), a slender spheroid (∗), a cylinder (△), a disk (◇), a cube (□), and a hemisphere (○). Small symbols correspond to $F=8$ and large symbols to $F=32$. Re≈5000. The solid line corresponds to the case of a sphere (Ref. 17) and the dotted line to a nonstratified sphere wake at early stages (Ref. 26).

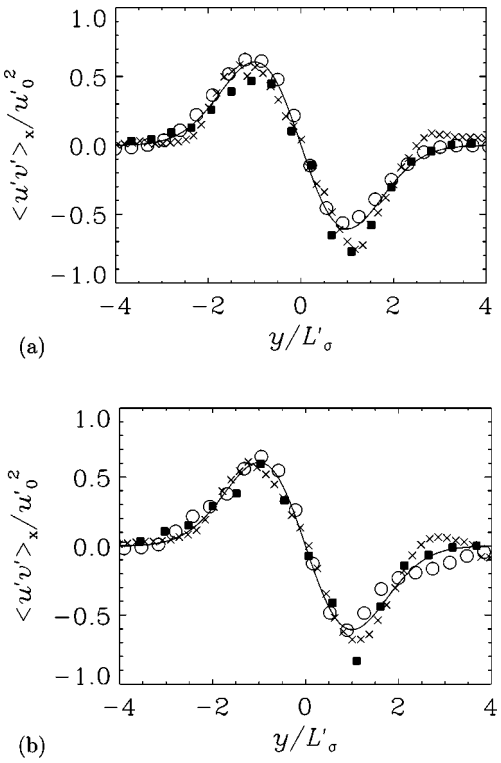

FIG. 7. Streamwise-averaged profile of the Reynolds stress $u'v'$ for the slender spheroid (a) and the cylinder (b) at three downstream distances: $x/D=170$ (■), $x/D=1000$ (○), and $x/D=5000$ (×). $F=32$ and Re≈5000. Solid lines correspond to the theoretical prediction (8) found in self-preserving wakes.

growth rate of L_σ, and can be explained by the fact that if the wake structure is self-preserved, λ_x is proportional to L_σ. Consequently, the Strouhal number should be larger for a streamlined object than for the sphere and slightly smaller for objects with sharp edges. This is clearly shown in Fig. 6(a) for the two different Froude numbers. Moreover, the results collapse very well when the Strouhal number is defined by the effective diameter ($\text{St}_{\text{eff}}=D_{\text{eff}}/\lambda$) instead of the diameter of the bluff body. Hence,

$$\text{St}_{\text{eff}}=0.65(x/D_{\text{eff}})^{-0.34}. \tag{6}$$

The results show that the global properties of the wake depend only on the amount of entrained fluid, which can be linked to the drag force. They are quite insensitive to the real shape of the bluff body and collapse very well using an effective diameter defined by (2) instead of the body's diameter. However, Bevilaqua and Lykoudis[10] have shown in a nonstratified wake that some memory could remain in the turbulent structure of the flow, even though the mean quantities follow the same evolution. The fluctuating quantities are examined in the next section.

IV. TURBULENT STRUCTURE OF THE WAKE

In three-dimensional turbulent wakes, Tennekes and Lumley[18] showed that the production of turbulence is due to the mean shear and can thus be modeled by an eddy viscosity, which should be independent of the bluff body. However, Bevilaqua and Lykoudis[10] showed that the amount of turbulence was three times smaller in the wake of a porous disk than in the wake of a sphere (of equal drag), at least for early stages ($x/D<110$). Their explanation was that the size of the turbulent eddies is smaller in the case of a porous disk, which would create a lower eddy viscosity.

In the theory of 3-D turbulence, the hypothesis of a constant eddy viscosity ν_T requires the cross-velocity fluctuations $\langle u'v'\rangle$ to be proportional to the mean shear:

$$\langle u'v'\rangle=\nu_T\frac{\partial U}{\partial y}. \tag{7}$$

The cross-fluctuation profile should thus be well fitted by the derivative of a Gaussian function:

$$\langle u'v'\rangle_x(y)=-u_0'^2\frac{y}{L_\sigma'}e^{-y^2/2L_\sigma'^2}, \tag{8}$$

characterized by an amplitude u_0' and a width L_σ'. If L_σ' is close to the mean wake width L_σ the amplitude u_0' defines a turbulent Reynolds number:

$$R_T=\frac{U_0L_\sigma}{\nu_T}=\frac{U_0^2}{u_0'^2}. \tag{9}$$

Figure 7 shows the cross-fluctuation profile for the cylinder and for the spheroid at three downstream distances. They are very well fitted by the function defined in Eq. (8) and Fig. 8(a) shows that the width of the fluctuations L_σ' is

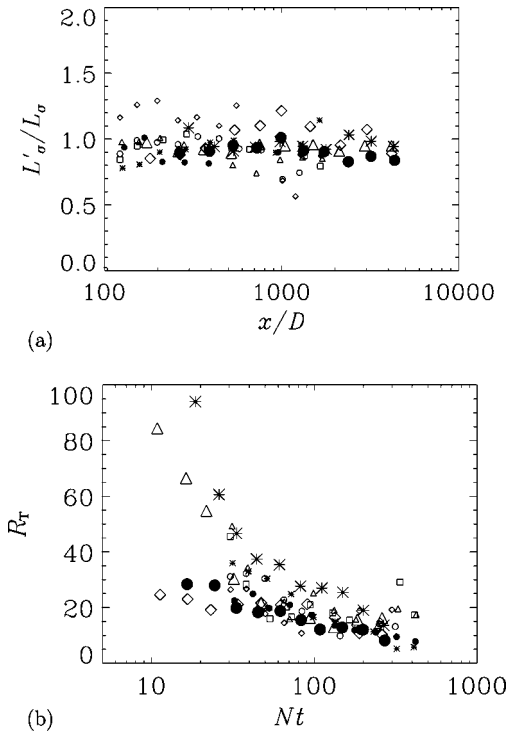

FIG. 8. Characteristics of the profile of the Reynolds stress $u'v'$ defined by Eq. (8). (a) Half-width L'_σ nondimensionalized by the wake width L_σ of the mean profile. (b) Turbulent Reynolds number $R_T=U_0^2/u_0'^2$. The objects are a sphere (●), a slender spheroid (∗), a cylinder (△), a disk (◇), a cube (□), and a hemisphere (○). Small symbols correspond to $F=8$ and large symbols to $F=32$. Re≈5000.

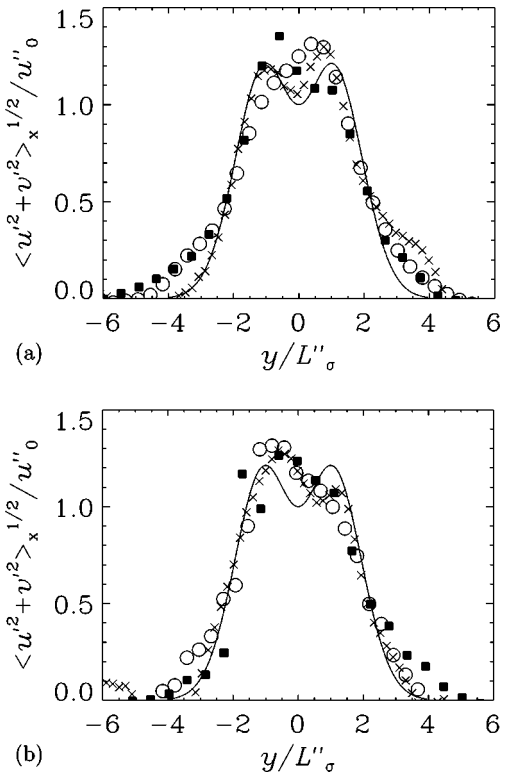

FIG. 9. Streamwise-averaged profile of the turbulent kinetic energy for the slender spheroid (a) and the cylinder (b) at three downstream distances: $x/D=170$ (■), $x/D=1000$ (○), and $x/D=5000$ (×). $F=32$ and Re≈5000. Solid lines correspond to the fitting function of Eq. (11).

very close to the mean wake width L_σ. This implies that the hypothesis of a constant eddy viscosity is valid not only at early stages, where the flow is close to two-dimensional, but also at late stages, where the structure of the flow is Q2-D.

To see if the eddy viscosity depends on the shape of the bluff body, Fig. 8(b) shows the turbulent Reynolds number for various objects. At early stages, R_T is three times higher for the cylinder and for the spheroid. This could be because the 3-D flows remember the shape of the bluff body, but it could also be because the flow is not yet at equilibrium, since this behavior is observed during the NEQ regime. Indeed, at late stages, all the results collapse to a constant value of the turbulent Reynolds number:

$$R_T \approx 15 \pm 5. \tag{10}$$

This value is in good agreement with the value $R_T \approx 20$ that can be deduced from the results of Spedding[22] and it is close to the values found for 3-D turbulent wakes, where R_T ranges from 5 to 30,[10] even though the physical mechanism might be slightly different. The memory of the initial shape of the bluff body is lost in the turbulent fluctuations, just as it was for the mean quantities.

A complete description of the fluctuating quantities must include the turbulent kinetic energy, which should be mainly contained in the horizontal components since, at late times ($Nt \gtrsim 50$), the vertical velocity is very small.[17] The horizontal turbulent kinetic energy can therefore be fit by a function characterized by an amplitude u''_0 and a width L''_σ:

$$(\langle u'^2+v'^2\rangle_x)^{1/2}(y)=u''_0\left(1+\frac{y^2}{L'^2_\sigma}\right)e^{-y^2/2L''^2_\sigma}. \tag{11}$$

Such a fitting function has been introduced by Dommermuth *et al.*,[23] to describe the results of Bevilaqua and Lykoudis[10] in the nonstratified sphere wake. The experimental profiles are shown in Fig. 9. The noise in the measurements is very high, and the profiles do not always present a double peak. However, the width of the fluctuating profile L''_σ is in good agreement with the width L_σ of the mean profile, as shown in Fig. 10(a). The amplitude u''_0 of the kinetic energy is shown in Fig. 10(b). As for the cross-fluctuations, the amplitude is slightly smaller for the cylinder and the spheroid at early stages, but at late stages, the amplitude of all bluff body data collapse onto

$$u''_0/U_0 \approx 0.25 \pm 0.05. \tag{12}$$

This value is in good agreement with values that can be derived from previous experimental ($u''_0/U_0 \approx 0.25$) and numerical ($u''_0/U_0 \approx 0.4$) results on the sphere.[22,23] Moreover, it is very close to the value found for the nonstratified wake of a porous disk ($u''_0/U_0 \approx 0.24$)[10] but smaller than for the case of a nonstratified sphere wake ($u''_0/U_0 \approx 0.6$).[10] However, this last result was obtained at relatively small downstream distances, where the equilibrium might not be settled yet.

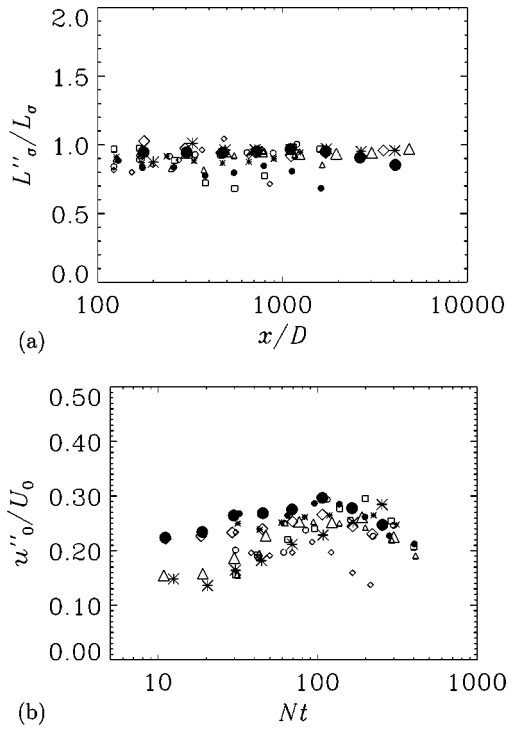

FIG. 10. Characteristics of the kinetic energy profile defined by Eq. (11). (a) Half-width L''_σ nondimensionalized by the wake width L_σ of the mean profile. (b) Amplitude u''_0 nondimensionalized by the velocity defect U_0. The objects are a sphere (●), a slender spheroid (*), a cylinder (△), a disk (◇), a cube (□), and a hemisphere (○). Small symbols correspond to $F=8$ and large symbols to $F=32$. Re≈5000.

V. DISCUSSION

Even though measurable differences have been observed in the wakes of different bluff bodies, the mean and fluctuating quantities can be easily collapsed using an effective diameter based on the drag coefficient. The wake does not remember the exact shape of the bluff body: it is only sensitive to the amount of fluid entrained behind the object. This idea suggests that the structure of the wake might be equivalent among objects and that its characteristics could be derived from this structure.

One may attempt to deduce the results of the previous sections from a simple 2-D model of the flow. The wake is imagined to be a row of alternate vortices of circulation Γ, with a Gaussian profile of vorticity $[\omega=\Gamma/\pi a^2 \exp(-r^2/a^2)]$ of core size a. Such a flow model and its stability has been studied in detail in the case of point vortices[24] and in the case of vortex patches,[25] but not in the case of Gaussian vortices. If the vortices are separated by λ_x in the x direction and by $2b$ in the y direction, using the periodicity of the flow, it can be shown that the mean profile is

$$U(y)=\frac{\Gamma}{2b}\left[\mathrm{erf}\left(\frac{y+b}{a}\right)-\mathrm{erf}\left(\frac{y-b}{a}\right)\right]. \tag{13}$$

This profile is close to a Gaussian for a/b close to 1 as is the case in the experiment, since a and b are of the order of the vortex sizes. The result, obtained by a two-dimensional model, is thus in good agreement with the global properties of the flow, although the flow is not two dimensional. This model does not predict the time evolution of wake width and velocity defect, which might be achieved by calculating the crossed fluctuations. However, a rough calculation shows that the crossed fluctuations vanish if the flow is exactly periodic. The model of the flow is therefore too simple to explain the velocity fluctuations and either some noise in the velocity field, or some aperiodicity of the flow should be taken into account.

ACKNOWLEDGMENTS

The support of ONR Grant No. N00014-96-1-0001 under Dr. L. P. Purtell and Dr. R. Joslin is most gratefully acknowledged.

[1] E. J. Hopfinger, "Turbulence in stratified fluids: A review," J. Geophys. Res. **92**, 5287 (1987).
[2] C. H. Gibson, "Internal waves, fossil turbulence, and composite ocean microstructure spectra," J. Fluid Mech. **168**, 89 (1986).
[3] J. R. Riley and M. P. Lelong, "Fluid motions in the presence of strong stable stratification," Annu. Rev. Fluid Mech. **32**, 613 (2000).
[4] J. T. Lin and Y. H. Pao, "Wakes in stratified fluids: A review," Annu. Rev. Fluid Mech. **11**, 317 (1979).
[5] Y. Xu, H. J. S. Fernando, and D. L. Boyer, "Turbulent wakes of stratified flow past a cylinder," Phys. Fluids **7**, 2243 (1995).
[6] Q. Lin, W. R. Lindberg, D. L. Boyer, and H. J. S. Fernando, "Stratified flow past a sphere," J. Fluid Mech. **240**, 315 (1992).
[7] J. M. Chomaz, P. Bonneton, and E. J. Hopfinger, "The structure of the near wake of a sphere moving horizontally in a stratified fluid," J. Fluid Mech. **254**, 1 (1993).
[8] G. R. Spedding, F. K. Browand, and A. M. Fincham, "Turbulence, similarity scaling and vortex geometry in the wake of a towed sphere in a stably stratified fluid," J. Fluid Mech. **314**, 53 (1996).
[9] G. R. Spedding, "The evolution of initially turbulent bluff-body wakes at high internal Froude number," J. Fluid Mech. **337**, 283 (1997).
[10] P. M. Bevilaqua and P. S. Lykoudis, "Turbulence memory in self-preserving wakes," J. Fluid Mech. **89**, 589 (1978).
[11] C. H. Gibson, C. C. Chen, and S. C. Lin, "Measurements of turbulent velocity and temperature fluctuations in the wake of a sphere," AIAA J. **6**, 642 (1968).
[12] M. S. Uberoi and P. Freymouth, "Turbulent energy balance and spectra of the axisymmetric wake," Phys. Fluids **13**, 2205 (1970).
[13] J. M. Chomaz, P. Bonneton, A. Butet, and E. J. Hopfinger, "Vertical diffusion in the far wake of a sphere moving in a stratified fluid," Phys. Fluids A **5**, 2799 (1993).
[14] S. I. Voropayev and I. A. Filippov, "Vortical track behind three-dimensional body moving in a stratified fluid," Morskoy Gydrofiz. Zhu. **6**, 62 (1985) (in Russian).
[15] A. M. Fincham and G. R. Spedding, "Low-cost high-resolution DPIV for turbulent flows," Exp. Fluids **23**, 449 (1997).
[16] S. I. Voropayev and S. A. Smirnov, "Vortex streets generated by a moving momentum source in a stratified fluid," Phys. Fluids **15**, 618 (2003).
[17] G. R. Spedding, "The streamwise spacing of adjacent coherent structures in stratified wakes," Phys. Fluids **14**, 3820 (2002).
[18] H. Tennekes and J. L. Lumley, *First Course in Turbulence* (MIT Press, Cambridge, MA, 1972).
[19] R. D. Blevins, *Applied Fluid Dynamics Handbook* (Van Nostrand Reinhold, New York, 1984).
[20] S. I. Voropayev, G. B. McEachern, H. J. S. Fernando, and D. L. Boyer, "Large vortex structures behind a maneuvering body in stratified fluids," Phys. Fluids **11**, 1682 (1999).
[21] S. A. Smirnov and S. I. Voropayev, "On the asymptotic theory of momentum/zero-momentum wakes," Phys. Lett. A **307**, 148 (2003).
[22] G. R. Spedding, "Anisotropy in turbulence profiles of stratified wakes," Phys. Fluids **13**, 2361 (2001).

[23]D. G. Dommermuth, J. W. Rottman, G. E. Innis, and E. A. Novikov, ''Numerical simulation of the wake of a towed sphere in a weakly stratified fluid,'' J. Fluid Mech. **473**, 83 (2002).
[24]P. G. Saffman, *Vortex Dynamics* (Cambridge University Press, Cambridge, 1992).
[25]D. Meiron, P. Saffman, and J. Schatzman, ''The linear two-dimensional stability of inviscid vortex streets of finite-cored vortices,'' J. Fluid Mech. **147**, 187 (1984).
[26]E. Achenbach, ''Vortex shedding from spheres,'' J. Fluid Mech. **62**, 209 (1974).